Mapping of mechanical properties of cement paste microstructures

[1]Howind T[*], [1]Hughes JJ, [1]Zhu W
[1] *University of the West of Scotland, Paisley, United Kingdom*
[2,3]Puertas F, [2,3]Goñi S, [2]Hernández MS, [2,3]Guerrero A
[2] *Eduardo Torroja Institute for Construction Science (IETcc), Spanish National Research Council (CSIC), Madrid, Spain*
[3] *Nanostructured and Eco-efficient Materials for Construction Unit, LABEIN-Tecnalia Associated Unit /IETcc, Spanish National Research Council (CSIC), Madrid, Spain*
[4]Palacios M
[4] *Instituto de Cerámica y Vidrio, Spanish National Research Council (CSIC), Madrid, Spain*
[3,5]Dolado JS
[5] *Centre for Nanomaterials Application in Construction (NANOC), LABEIN-Tecnalia, Bilbao, Spain*

Abstract
The presented study is related to the EU 7th Framework Programme CODICE (COmputationally Driven design of Innovative CEment-based materials). The main aim of the project is the development of a multi-scale model for the computer based simulation of mechanical and durability performance of cementitious materials.
This paper reports results of micro/nano scale characterisation and mechanical property mapping of cementitious skeletons formed by the cement hydration at different ages. Using the statistical nanoindentation and micro-mechanical property mapping technique, intrinsic properties of different hydrate phases, and also the possible interaction (or overlapping) of different phases (e.g. calcium-silcate-hydrates) has been studied. Results of the mapping and statistical indentation testing appear to suggest the possible existence of more hydrate phases than the commonly reported LD and HD C-S-H and CH phases.

Originality
Through the characterisation of the different calcium silicate hydrates (C-S-H) there is evidence for the possible presence of more than the common C-S-H and CH phases. The new phase identified could be created by the overlapping of outer and inner C-S-H products with outer C-S-H products during the hydration process. Similar observations have been made by the modellers involved in the European CODICE research project during their work at modelling of the hydration of cementitious materials.

Chief contributions
The composition and strength of hydrated pastes made from different calcium silicates were determined in a sub-micro/nanoscale scale by using the nanoindentation technique and electron microscopy. Especially the nanoindentation results delivered evidence for the possible existence of more C-S-H phases than commonly reported. It seems possible that the new phases were formed during the hydration by the overlapping of and outer C-S-H products.

Keywords: *Cement, Nanoindentation, Mapping, Young's modulus, Hardness*

[*] Corresponding author: Email: torsten.howind@uws.ac.uk; tel. +44 141 849 4089

Introduction

The presented study is related to the EU 7th Framework Programme CODICE (COmputationally Driven design of Innovative CEment-based materials). The project's main aim is to development of a multi-scale model for the computer based simulation of mechanical and durability performance of cementitious materials. At different stages of the model development, experimental data obtained by nanoindentation measurements of hydrated pastes of typical Portland cement were required to calibrate or validate the model.

Previous work (e.g. Constantinides *et al.*, 2007; DeJong *et al.*, 2007 and Zhu *et al.*, 2007) has shown that nanoindentation can be used to map mechanical properties of multiphase materials. The spatial resolution of the nanoindentation test allows assessing the linkage between microstructure and micromechanical performance. This paper reports a study to assess nanoindentation mapping of mechanical properties of white ordinary Portland cement (WOPC) paste hydrated for 7 days and pure synthetic β-C_2S hydrated for 90 days. Besides, the microstructures of both WOPC and β-C_2S were studied obtained from scanning electron microscopy (SEM), thermal analyses, mercury intrusion porosimetry, BET-N_2 specific surface area (SSA) and ^{29}Si MAS NMR. The results appeared to show indications of the existence of more hydrate phases than the commonly reported phases, such as CH and low density (LD), high density (HD) calcium silicate hydrates (C-S-H). The comparative microstructural study of WOPC and β-C_2S pastes revealed very close microstructures.

Materials and experimental methods

Synthetic β-C_2S and typical CEM I 52.5N white ordinary Portland cement provided by Italcementi Group (Bergamo, Italy) was used with a fixed water to cement ratio (w/c) of 0.40. The pastes were cast in cylindrical moulds (∅ 15 mm) and compacted using a vibrating table. The specimens were demoulded 24 hours after casting and wrapped in kitchen foil and stored at room temperature (20±3°C). At selected ages (e.g. 7 and 90 days) the hydration was stopped using acetone. For the nanoindentation experiments small discs with a thickness of approximately 10 mm were cut from cement paste cylinders and embedded in resin. This was followed by a resin impregnation necessary to support the weak microstructure of cement paste at early stages of hydration. Afterwards subsequent grinding and polishing steps down to ¼ μm were performed to obtain the final test specimens (∅ 30×20 mm). Alcohol or oil-based polishing slurries and lubricants were used throughout preparation process to avoid further cement hydration and possible dissolution of hydrate phases.

Table 1: Composition of the white cement in mass percentage (components smaller than 1% are not included)

SiO_2	Al_2O_3	CaO	MgO	SO_3	Na_2O	MnO	LOI	Density	Blaine
19.39	3.26	67.89	1.75	3.63	1.28	1.75	1.82	3.08 g/cm^3	2958.47 cm^2/g

The methodology and operating principle for the nanoindentation technique have been reviewed and presented in detail elsewhere (e.g. Oliver *et al*., 1992, 2004; Constantinides *et al.*, 2003; Ulm *et al.*, 2007; Sorelli *et al.*, 2008). As a load is applied to an indenter in contact with the surface of a specimen, an indent is produced consisting of elastic and plastic deformation. The recovery of the elastic deformation occurs at the start of unloading. Thus, analysing the initial part of the unloading data allows the determination of the Young's modulus, *E*, and hardness, *H*, for the indented area.

The nanoindentation apparatus used in this study was an Agilent Nano Indenter® G200 fitted with a Berkovich indenter tip. A progressive multistep indentation testing with two load-unload cycles were performed at each test point. The unloading data of the second cycle ($h_p \approx 200$ nm) were used to determine the modulus and hardness values (Figure 1).

Results obtained from mechanical properties mapping form the base for a future computational driven model on hydration and mechanical performance of cementitious materials. Thus an area, roughly

100 x 100 μm², was chosen for the nanoindentation testing, which is similar to the basic representative computational unit of the proposed model.

Immediately after the nano-indentation experiment the tested sample area was studied using a High Resolution Field-Emission Scanning Electron Microscope (HR FE-SEM Hitachi S-4100) in conjunction with energy-dispersive spectroscopy (EDS) analysis was used to determine qualitatively and quantitatively the mineral compositions (using cobalt gain calibration was applied) of the tested area. These enable correlation of micromechanical properties and the corresponding microstructure (e.g. morphology), as well as the composition of the involved phases to be established.

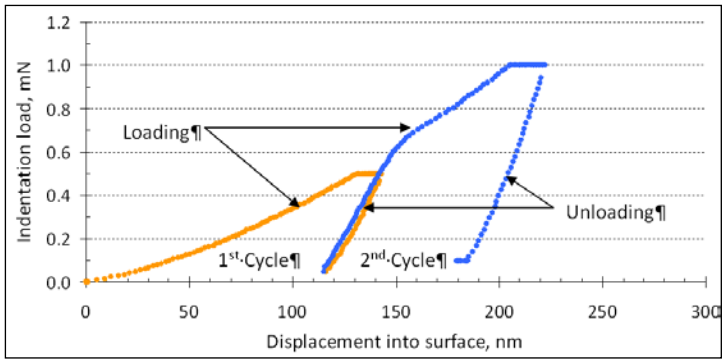

Figure 1: Typical *P* - *h* curve of a two-step nano-indentation test

^{29}Si MAS NMR was likewise used to monitor the mean chain length (MCL) of the C-S-H gels formed. A Bruker MSL400 spectrophotometer operating at 79.49 MHz was used ad tetramethyl silane (TMS) as external standard for the ^{29}Si spectra. Spectral analyses were performed using Winfit software (Bruker). Component intensity, position and line width were determined with a standard interactive least squares method. The scanning electron microscope used was a JOEL JSM 5400 model, fitted with a solid-state backscattered detector and a LINK-ISIS EDX microanalyser. Surface area measurements were made by the BET multipoint method (Model ASAP 2010, Micromeritics Instrument Corp., Norcross, GA), using N2-77 K gas. Thermal analyses were carried out with a Netxsch STA 409 simultaneous thermal analyser fitted with a Data Acquisition Systems 414/1 programmer. Samples (maximum amount accommodated by the crucible) were heated to 1050 ºC at a rate of 4 ºC min^{-1} in an inert atmosphere (N_2) and subsequently cooled at 10 ºC min^{-1}, Total porosity and pore size distribution of pastes were found with Hg intrusion porosimetry (MIP) on a Micromeritics 9320 porosimeter.

Comparative microstructural study

The main microstructural characteristics of both WOPC hydrated for 7 days and β-C_2S hydrated for 90 days are presented in Table 2. The degree of hydration has been calculated from thermal analyses according to a previous work (Goñi *et al*., 2010). Despite the great difference of hydration time, the hydration degrees are quite similar: 0.55 and 0.57 for β-C_2S and WOPC, respectively. As a consequence, the values of the rest of microstructural parameters are also similar.

Table 2: Microstructural parameters of β-C_2S hydrated for 90 days and WOPC hydrated for 7 days

	β-C_2S	WOPC
Degree of Hydration (a)	0.55	0.57
Surface area (m²/g)	10	10
Porosity (mL/100g)*	16	14
Bulk density (g/mL)*	1.7	1.7
Mean chain lengthy (MCL)	3.9	3.7

* Porosity and bulk density measured by MIP

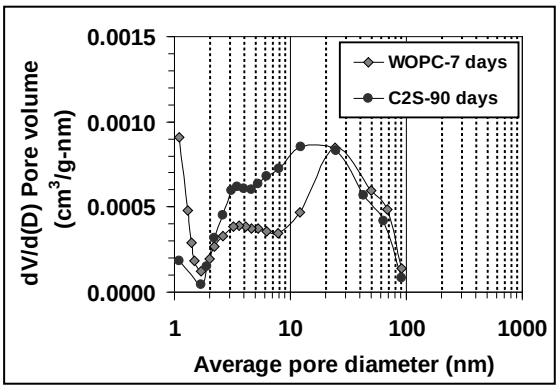

Figure 2: Pore-size distribution of WOPC and β-C_2S pastes

Nevertheless, differences appear in the distribution of the nano-porosity (Figure 2), where the bimodal distribution (with maxima at 3 - 5 nm and 10 - 20 nm) shows higher proportion of small pores in the case of the β-C_2S. This seems to be in a good agreement with the SEM results as they appear to show for β-C_2S a more open fibrous morphology of C-S-H gel particles compared to WOPC. As an example, the morphologies of the main components of the microstructures: portlandite and C-S-H gel are presented in Figure 3.

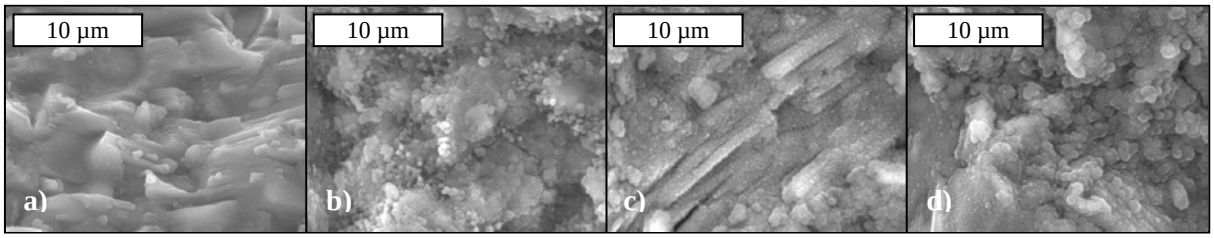

Figure 3: SEM micrographs of portlandite and C-S-H gel from β-C_2S paste (a) and (b) and WOPC (c) and (d)

Mapping of mechanical properties

Limited tests were initially carried out on a synthetic β-C_2S sample with 90 days of hydration. A grid of 10 x 8 indentation test points with an indent spacing of 10 µm was used. The results of 80 indents are shown in Figure 4. There appears to be a very good agreement between mechanical properties and the microstructure of the corresponding test area surface (Figure 4a) obtained from SEM. The unhydrated or partially hydrated cement clinker particles indentified as white or lighter grey shade in the SEM image have clearly much higher values of Young's modulus and hardness in the mechanical properties maps. The hydrate phases, e.g. CH and C-S-H, seen as dark grey shade show modulus and hardness values in a range of 20 - 40 GPa and 0.4 - 1.6 GPa respectively. Young's modulus values lower than 20 GPa are believed to be due to surface defects or porosity in the sample. From the SEM images it seems not possible to differentiate between the different C-S-H phases.

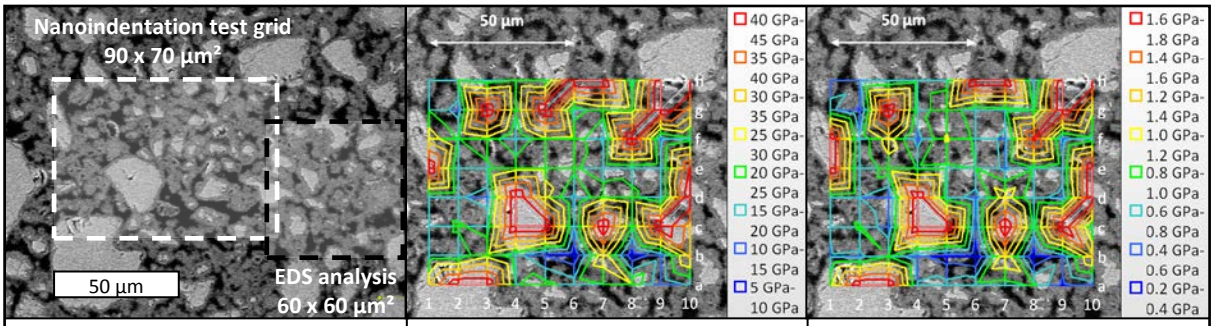

Figure 4: SEM image and mechanical properties maps of the tested area (90 days C_2S paste)

In order to provide sufficient information on the distribution of the different C-S-H phases more work on the EDS elemental mapping was undertaken. Figure 5 shows elements maps of calcium and silicate, obtained by EDS. An area with more hydration phases, adjacent to the nanoindentation area on the SEM image (Figure 3) has chosen for the analysis. From the element maps in Figure 5, the unhydrated cement clinker particles can be easily identified by high contents of calcium and silicate whereas Portlandite (CH) is denoted by the only presence of calcium. The C-S-H phases were found to have relatively lower contents of both Ca and Si. The ratios of Ca/Si at various points were analysed, but still will not be able to provide a reliable measure to differentiate the different C-S-H phases, possibly because the main differences of the various C-S-H phases were in their densities not in their compositions.

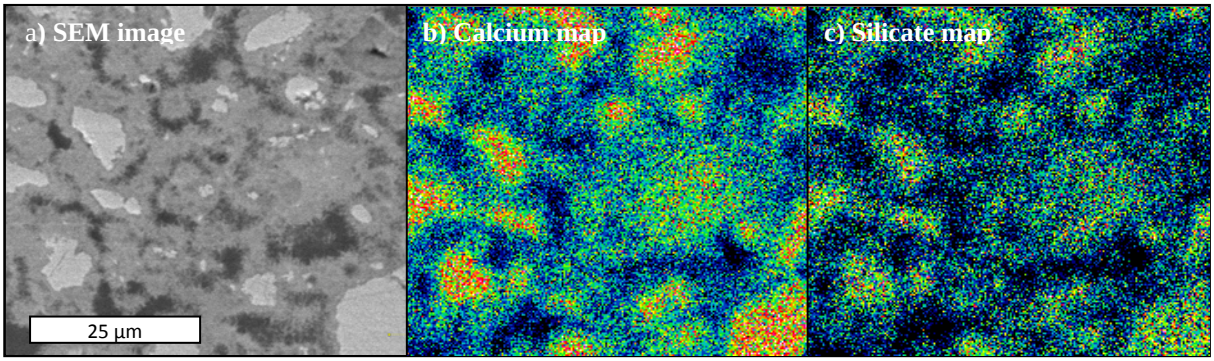

Figure 5: Detail of the SEM image (seen in Figure 4) and element distribution maps from the EDS analysis; limited differentiation between different hydrate phases, such as unhydrated clinker, CH and C-S-H

A statistical or grid nanoindentation experiment involving large number of test points has shown to provide micromechanical properties and volume proportions of different C-S-H phases (e.g.; Constantinides *et al.*, 2007; Zhu *et al.*, 2007; Ulm *et al.*, 2010 and). It was thus decided to carry out the subsequent testing on a white Portland cement paste using 900 test points and a much smaller indent spacing of 3 µm (Figure 6a). Figure 6b and Figure 6c show the mechanical properties maps for the 7-day hydrated white cement paste. Similar to the initial study on C_2S, the mechanical properties maps show good correlation with the SEM image.

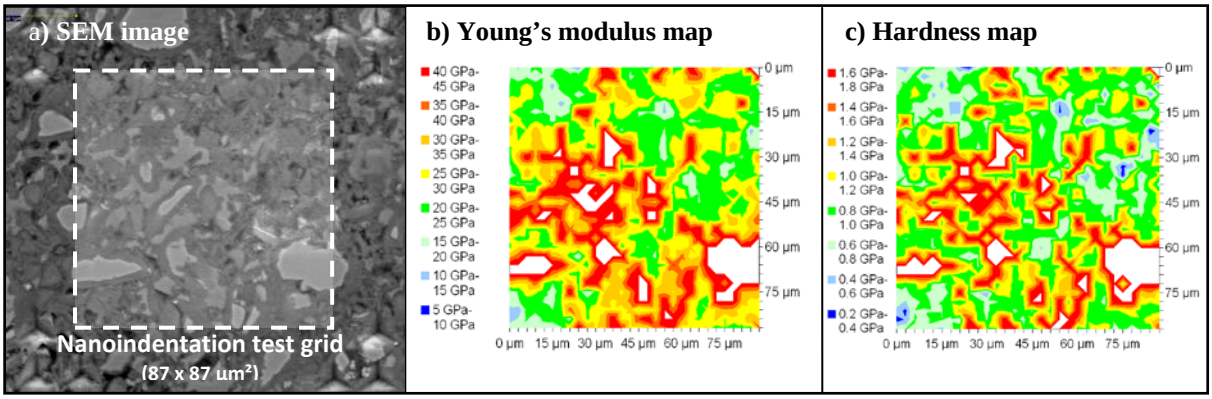

Figure 6: SEM image of the tested area (900 indents) in cement paste and corresponding mechanical properties maps for *E* and *H*

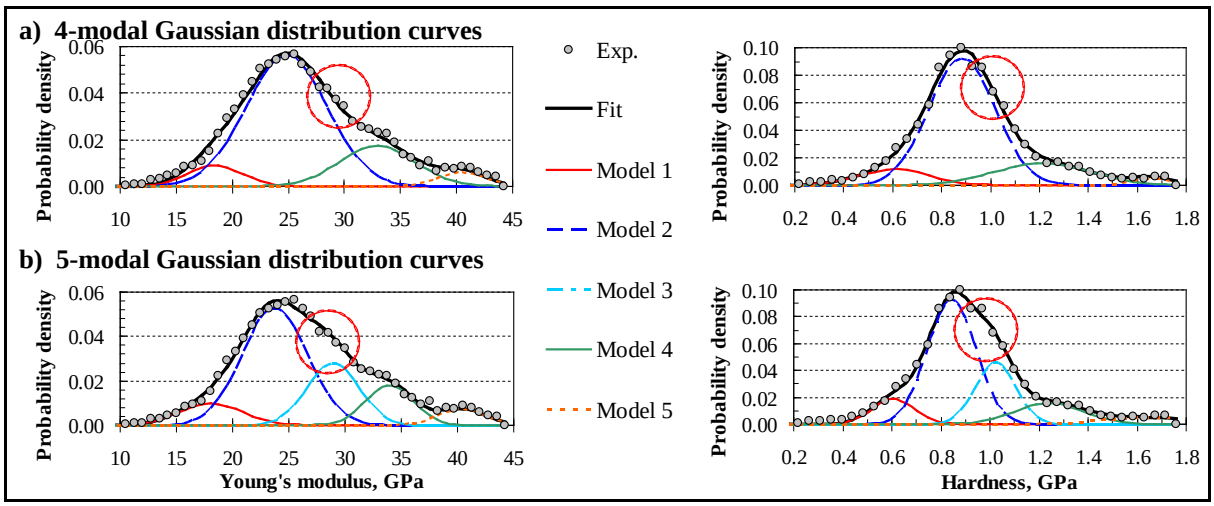

Figure 7: Probability density vs. Young's modulus and Hardness diagrams obtained from 900 indentions with 4- and 5-modal Gaussian distribution curves

Statistical analysis of the large number of indentation test results obtained (900 indents) was carried out to extract the specific mechanical properties of each individual phase in the tested area using the deconvolution technique presented previously (Constantinides *et al.*, 2003; Ulm et al, 2007; Zhu *et al.*; 2007; Sorelli *et al.*, 2008). Figure 7 presents the statistical distribution of both Young's modulus and hardness test results and the possible model fits with multi-modal Gaussian distribution curves (4-modal in Figure 7a and 5-modal in Figure 7b) within the range of mechanical properties for the hydration phases. The results of the specific mechanical properties of the individual hydrate phases of tested white Portland cement after 7 days of hydration are summarised in Table 3.

Table 3: *E* and *H* values extracted from two different model fits for the individual hydrate phases indentified (white Portland cement paste, 7 days of hydration)

	4-modal Gaussian distribution curves			**5-modal Gaussian distribution curves**		
	Young's modulus	Hardness	Surface fraction	Young's modulus	Hardness	Surface fraction
Model 1: *loose-packed C-S-H*	18.45 ±2.45GPa	0.61 ±0.14GPa	7.4 to 9.4%	18.09 ±2.78GPa	0.61 ±0.09GPa	9.2 to 9.2%
Model 2: *LD C-S-H*	24.84 ±3.62GPa	0.88 ±0.13GPa	68.4 to 70.4%	23.76 ±2.89GPa	0.84 ±0.10GPa	51.2 to 51.7%
Model 3: *Overlapping C-S-H*				28.95 ±2.29GPa	1.02 ±0.08GPa	21.0 to 21.5%
Model 4: *HD C-S-H*	32.92 ±3.36GPa	1.21 ±0.20GPa	17.8 to 19.8%	33.96 ±2.13GPa	1.24 ±0.14GPa	12.3 to 12.8%
Model 5: *CH*	40.52 ±2.14GPa	1.66 ±0.08GPa	2.3 to 4.3%	40.36 ±2.08GPa	1.66 ±0.20GPa	5.2 to 5.7%

The probability density curve of the experimental data shows clearly more than 3 peaks of the common hydrate phases (LD C-S-H, HD C-S-H, CH). One of the additional peaks at the beginning could be related to a C-S-H phase of reduced density. Ulm *et al* (2007) and Zhu *et al* (2009) already propagated the existence of a so-called loose-packed C-S-H. Finding an explanation for the occurrence of peaks between LD C-S-H and HD C-S-H appears to be rather difficult. Based on the nanoindentation results presented in Figure 7 and particularly mainly other test results which have yet to be published, it appears that another peak could be identified between the LD C-S-H and HD C-S-H peaks as shown in Figure 7b, representing the overlapping C-S-H phase in Table 1. Work is still on-going to characterise differences in chemical composition and packing density of the various hydrate phases within the indented area so as to link microstructural features with phase properties obtained from the mechanical performance mapping.

Nevertheless, the mechanical property values extracted for the common C-S-H phases are in very good agreement with the values obtained for a 28-day hydrated cement specimen (without resin impregnation) and reported by Acker (2001) (e.g. $E_{\text{LD C-S-H}}$=20.0±2.0 GPa, and $E_{\text{HD C-S-H}}$=31.0±4.0 GPa), by Constantinides *et al.* (2003) (e.g. $E_{\text{LD C-S-H}}$=21.7±2.2 GPa, and $E_{\text{HD C-S-H}}$=29.4±2.4 GPa) and Zhu *et al.* (2009) (e.g. $E_{\text{loose-packed C-S-H}}$=18.1 GPa, $E_{\text{LD C-S-H}}$=24.4 GPa, and $E_{\text{HD C-S-H}}$=31.4 GPa). This also supports the argument that the elastic properties of the different C-S-H phases are intrinsic to cement paste.

Conclusion

1. Despite the different time of hydration: 90 days for β-C_2S and 7 days for WOPC, very similar microstructural characteristics were found by the different techniques.
2. The results of this study showed that nanoindentation mapping of mechanical properties provides a useful tool to link with microstructure and modelling studies for improved understanding of cementitious materials.
3. The results indicate the existence of a loose-packed C-S-H as previously proposed by a few other researchers.

4. Results of the mapping and statistical indentation testing appear to suggest the possible existence of one additional C-S-H phase with mechanical properties between LD C-S-H and HD C-S-H, possibly as a result of an overlapping of the C-S-H phases.

Acknowledgements

Firstly, the authors gratefully acknowledge the financial support of the CODICE project by the European Commission under project FP7-NMP3-SL-2008-214030. Furthermore, we would like to express greatest thanks for help and support to all the other partners within the research project: Technische Universiteit Delft (The Netherlands), Rheinische Friedrich-Wilhelm-Universität Bonn (Germany), CTG S.p.A. (Italy), Morteros y Revocos BIKAIN, S.A. (Spain) and BASF SE (Germany).

Refrences

Acker, P., 2001. Micromechanical analysis of creep and shrinkage mechanisms. In: Ulm, F.J., Bazant, Z.P., Wittmann, F.H., editors. *Creep, shrinkage and durability mechanics of concrete and other quasi-brittle materials*, Cambridge, MA. Oxford, UK: Elsevier.

Constantinides, G., Ulm, F.-J. and Van Vliet, K., 2003. On the use of nanoindentation for cementitious materials. *Materials and Structures* 36, 191-196.

Constantinides, G. and Ulm, F.-J., 2007, The nanogranular nature of C-S-H. *Journal of the Mechanics and Physics of Solids* 55, 64-90.

DeJong, M.J. and Ulm F.-J., 2007. The nanogranular behavior of C-S-H at elevated temperatures (up to 700 °C). *Cement and Concrete Research* 37, 1-12.

Goñi S., Puertas F., Hernández M.S., Palacios M., Guerrero A., Dolado J.S., Zanga B. and Baroni F., 2010. Quantitative study of hydration of C_3S and C_2S by thermal analysis. Evolution and composition of C-S-H gels formed. *Journal of Thermal Analysis and Calorimetry*. Published online: 06 May 2010. DOI: 10.1007/s10973-010-0816-7.

Oliver, W.C. and Pharr G.M., 1992. An improved technique for determining hardness and elastic modulus using load and displacement sensing indentation experiments. *Journal of Materials Research* 7, 1564-1583.

Oliver, W.C. and Pharr G.M., 2004. Measurement of hardness and elastic modulus by instrumented indentation: Advances in understanding and refinements to methodology. *Journal of Materials Research* 19, 3-20.

Ulm F., Vandamme M., Bobko C., Ortega J,A., Tai, K. and Ortiz, C., 2007. Statistical indentation techniques for hydrated nanocomposites: concrete, bones and shale. *Journal of the American Ceramic Society* 90(9), 2677-2692.

Ulm, F.-J., Vandamme, F., Jennings, H.M., Vanzo, J., Bentivegna, M., Krakowiak, K.J., Constantinides, G., Bobko, C.P. and Van Vliet, K.J., 2010. Does microstructure matter for statistical nanoindentation techniques?. *Cement & Concrete Composites* 32, 92-99.

Sorelli, L., Constantinides, G., Ulm, F.-J. and Toutlemonde, F., 2008. The nano-mechanical signature of Ultra High Performance Concrete by statistical nanoindentation techniques, *Cement and Concrete Research* 38, 1447-1456.

Zhu, W., Hughes, J., Bicanic, N. and Pearce, C.J., 2007. Micro/Nano-scale mapping of mechanical properties of cement paste and natural rocks by nanoindentation. *Materials Characterization* 11, 1189-1198.

Zhu, W., Fonteyn, M.T.J, Hughes J. and Pearce, C., 2009. Nanoindentation study of resin impregnated sandstone and early-age cement paste specimens. In: Bittnar, Z., Bartos, P.J.M., Němeček, J., Šmilauer, V., Zeman, J., Editors. *Nanotechnology in Construction 3*, Springer Berlin Heidelberg.